

Effect of sample composition on the separation efficiency of isotachophoresis

TAKESHI HIROKAWA*, YASURO YOKOTA^a and YOSHIYUKI KISO

Applied Physics and Chemistry, Faculty of Engineering, Hiroshima University, Kagamiyama 1, Higashi-hiroshima 724 (Japan)

ABSTRACT

In order to clarify the effect of the sample composition on the separation efficiency of isotachophoresis, approximate equations expressing the resolution time of strong electrolytes were derived. The transient two-component mixed zone formed in the separation process of a three-component mixture was simulated by varying the molar amount and the mobility of the third component. It was apparent that the resolution time of two components of interest was increased with the addition of the other components, owing to the change in the potential gradient of the two-component mixed zone. The magnitude of the delay was especially large when the mobility of the added component was close to that of the two components of interest. The increase in resolution time was evaluated for the separation of mixtures of up to six equimolar components. The present simulation was confirmed by analysing the actual separation process using a scanning ultraviolet spectrophotometric detector.

INTRODUCTION

The driving force of isotachophoretic separation is the different migration velocities of separands in the transient mixed zones [1,2]; a large difference in these migration velocities means efficient separation. As the electrophoretic velocity is expressed by the product of the effective mobility of an ion and the potential gradient of its zone, the resolution time of the mixed zone must depend on both factors.

In the optimization of isotachophoretic separations, however, the effect of effective mobility on the separation efficiency has been emphasized [1–3]. In fact, the optimization of the pH of the leading electrolyte is undoubtedly very important, and this is obtained straightforwardly from the pH dependence of the effective mobility of weak electrolytes. Mikkers *et al.* [4,5] have given a theoretical elucidation of the effect of pH on the separation efficiency of two-component mixtures. The separability of a two-component mixture was discussed in relation to the pH of the operational system considering zone stability by Bocek and Gebauer [6]. It was also reported that the pH of the sample solution affects the separation efficiency [4,5], although not so seriously

* Present address: Mitsubishi Paper Mills Ltd., Tsukuba Research Laboratories, Tsukuba, Ibaraki, Japan.

[7]. The dynamics of the isotachophoretic separation of two-component mixtures was reviewed by Thormann [8].

In addition to straightforward factors such as effective mobility, however, we have suggested another important factor that affects the separation efficiency, namely the composition of the sample solution [9]. This was based on the fact that the resolution time of a two-component mixed zone formed in the isotachophoretic separation process of a three-component mixture was longer than that of the equivalent two samples being separated independently. Although this phenomenon has been confirmed experimentally [9], it was not apparent how the separation efficiency was affected by the addition of other separands to the original two-component mixture. This is an important problem for practical samples, especially from the viewpoint of the optimization of their separation.

In order to elucidate this phenomenon, several equations were derived to express the resolution time of strong electrolytes, which are free from dependence of the effective mobility on pH. The separation process of a mixture of SPADNS, monochloroacetic acid, picric acid and 2,4-dihydroxybenzoic acid was analysed to examine our conclusions based on computer simulation. A new scanning ultraviolet (UV) spectrophotometric detection system was utilized for the direct observation of the separation process [10]. The observed tendency of the separation efficiency was compared with the simulated data.

THEORETICAL

Assume a two-component mixture consisting of strong electrolytes. The separand ions, A and B, are monovalent and ion A is more mobile than ion B. The resolution time of the mixed zone AB can be expressed as follows [4,5]:

$$t_{\text{res,AB}} = \frac{l_A}{V_{\text{ITP}} - V_{\text{A/AB}}} = \frac{l_A}{E_A \bar{m}_A - E_{\text{AB}} \bar{m}_{\text{B,AB}}} \quad (1)$$

where l_A is the zone length of the separand A in a separation tube at the steady state, V_{ITP} the isotachophoretic velocity, $V_{\text{A/AB}}$ the velocity of the boundary between zones A and AB, E_A the potential gradient of zone A at the steady state, \bar{m}_A the effective mobility of ion A in zone A at the steady state, E_{AB} the potential gradient of the mixed zone AB and $\bar{m}_{\text{B,AB}}$ the effective mobility of ion B in zone AB. The zone length l_A is linearly proportional to the sample amount [1-3], which is expressed as follows using the time-based zone length t_A [3,11] and the isotachophoretic velocity $E_A \bar{m}_A$:

$$l_A = t_A E_A \bar{m}_A = \frac{Fn_A}{i} (1 + m_Q/m_A) E_A \bar{m}_A \quad (2)$$

where F is the Faraday constant, n_A the molar amount of component A, i the migration current and m_Q the mobility of the counter ion as the pH buffer in the steady zone of A. Combination of eqns. 1 and 2 yields

$$t_{\text{res,AB}} = \frac{Fn_A}{i} (1 + m_Q/m_A) \frac{E_A \bar{m}_A}{(E_A \bar{m}_A - E_{\text{AB}} \bar{m}_{\text{B,AB}})} \quad (3)$$

As E_A and \bar{m}_A are quantities at the steady state, they are independent of coexisting components. Also, in this particular case of a strong electrolyte, $\bar{m}_{B,AB}$ will have almost the same value as the effective mobility of ion B^a at the steady state and will not be affected by the sample composition. Therefore, the possibility of causing a change in $t_{res,AB}$ must result from a change in E_{AB} or the specific conductivity of the mixed zone. These values may be affected by the molar amount and the mobility of the coexisting ionic components in a sample. Our purpose in this section is to derive the equations that express how E_{AB} and the resolution time are affected by the sample composition.

From the moving boundary equation [12], E_{AB} is exactly correlated with E_A as follows:

$$E_{AB} = \frac{\bar{m}_A C_A^t}{\bar{m}_{A,AB} C_{A,AB}^t + \bar{m}_{B,AB} (C_A^t - C_{A,AB}^t)} \cdot E_A \quad (4)$$

where $\bar{m}_{A,AB}$ is the effective mobility of the separand A in the zone AB, C_A^t the total molar concentration of A in the partly separated steady-state zone and $C_{A,AB}^t$ is that in the mixed zone AB.

The potential gradient of the mixed zone is closely related to the composition of the zone. The concentration ratio of the two components in the mixed zone is expressed as follows using the concentration and mobility in the injected solution (I) [13]:

$$\frac{C_{B,AB}^t}{C_{A,AB}^t} = \frac{\bar{m}_{A,AB} \bar{m}_{B,I} C_{B,I}^t}{\bar{m}_{B,AB} \bar{m}_{A,I} C_{A,I}^t} \quad (5)$$

In the present equimolar case for strong electrolytes, the ratio is regarded as unity. Further, as a first approximation, the following equation is valid for the two-component mixed zone AB:

$$C_{A,AB}^t + C_{B,AB}^t = C_A^t \quad (6)$$

$$C_{A,AB}^t = C_A^t / 2 \quad (7)$$

As the separands are strong electrolytes, the effective mobilities of ions A and B in the mixed zone may be regarded as being equal to those at the steady state, \bar{m}_A and \bar{m}_B , if we neglect the difference in the ionic strength:

$$\bar{m}_{A,AB} = \bar{m}_A; \bar{m}_{B,AB} = \bar{m}_B \quad (8)$$

By inserting eqns. 5–8 into eqn. 4, one can obtain a very simplified expression for the potential gradient of the mixed zone for the two-component mixture:

$$E_{AB(2)} = \frac{2\bar{m}_A}{\bar{m}_A + \bar{m}_B} \cdot E_A \quad (9)$$

^a In anionic analysis, the relation $\text{pH}_L < \text{pH}_A < \text{pH}_{AB} < \text{pH}_B$ is usually valid, while the separands are monovalent strong electrolytes. Therefore, this relationship is no longer a good approximation for weak electrolytes.

where the number 2 in parentheses is the number of components in the sample mixture. Then eqn. 3 is reduced to the following form:

$$t_{res,AB}(2) = \frac{Fn_A}{i} (1 + m_Q/m_A) \frac{\bar{m}_A + \bar{m}_B}{\bar{m}_A - \bar{m}_B} \quad (10)$$

Apparently from eqn. 10, the resolution time is the time-based zone length multiplied by the ratio of the sum to the difference of the mobilities of separands. With strong electrolytes, the effective mobility in eqn. 10 can be replaced with the absolute mobility. Mikkers *et al.* [4] concluded that the ratio of the separand mobilities is one of the most important factors affecting the separation efficiency. The same conclusion can be derived from eqn. 10. We left eqn. 10 as it was, because it seemed to be straightforward.

Table I gives the resolution times of several model anions evaluated by the approximate eqn. 10, together with those simulated exactly. The mobility of ion A was $60 \cdot 10^{-5}$ and $30 \cdot 10^{-5} \text{ cm}^2 \text{ V}^{-1} \text{ s}^{-1}$ and the mobility difference between ions A and B was in the range $1 \cdot 10^{-5}$ – $10 \cdot 10^{-5} \text{ cm}^2 \text{ V}^{-1} \text{ s}^{-1}$. The leading ion was 10 mM chloride and the mobility was $79.08 \cdot 10^{-5} \text{ cm}^2 \text{ V}^{-1} \text{ s}^{-1}$. The pH of the leading electrolyte was 6 and the pH buffer used was histidine ($m_Q = 29.6 \cdot 10^{-5} \text{ cm}^2 \text{ V}^{-1} \text{ s}^{-1}$, $pK_a = 6.04$). The validity of eqn. 10 as a first approximation is obvious from Table I, as the deviation is less than 10%.

Figs. 1 and 2 were plotted for convenience of a rapid calculation of the resolution time of a two-component mixed zone, where the mobility of the first appearing separand (m_A) was varied in the range $15 \cdot 10^{-5}$ – $75 \cdot 10^{-5} \text{ cm}^2 \text{ V}^{-1} \text{ s}^{-1}$ and the mobility difference in the range 0 – $10 \cdot 10^{-5} \text{ cm}^2 \text{ V}^{-1} \text{ s}^{-1}$. Fig. 1 shows the exactly simulated resolution time in the range 0–2000 s. In Fig. 2, time scale was expanded. The other operational conditions for Figs. 1 and 2 were the same as those in Table I. Apparently from Figs. 1 and 2, the resolution time decreased with decrease in the

TABLE I

EXACTLY SIMULATED AND APPROXIMATELY EVALUATED RESOLUTION TIMES OF TWO-COMPONENT MIXTURES OF SEVERAL MODEL ANIONS

m_A, m_B = Absolute mobilities of model anions (A and B) ($\times 10^5 \text{ cm}^2 \text{ V}^{-1} \text{ s}^{-1}$). Amount of separands = 10 nmol. Migration current = 100 μA . Approximate resolution time was evaluated using eqn. 10. Leading electrolyte: 10 mM HCl–histidine (pH 6).

m_A/m_B	Resolution time (s)		
	Exact	Approximate	Difference (%)
60/59	1614	1715	6.3
60/58	803	850	5.9
60/55	316	331	4.7
60/50	153	158	3.3
30/29	1050	1131	7.7
30/28	521	556	6.7
30/25	203	211	3.9
30/20	97	96	–1.0

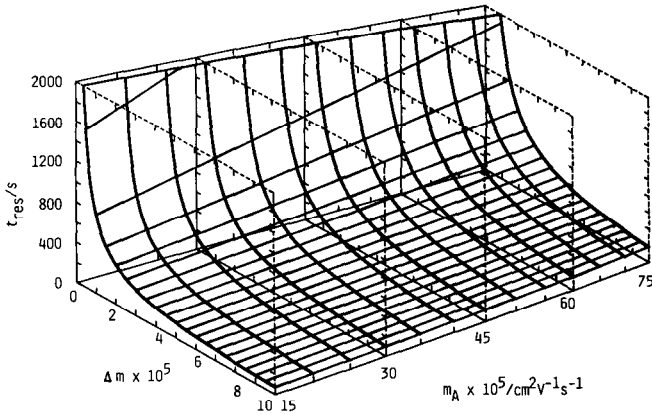


Fig. 1. Resolution time of an equimolar two-component mixture of model anions, A and B. m_A = Mobility of the first appearing ion; Δm = mobility difference between the separands; t_{res} = resolution time of the mixed zone. The amount of each separand was 10 nmol. Leading electrolyte, 10 mM HCl-histidine (pH 6); migration current, 100 μA .

mobility of the first appearing separand, when the mobility difference of the separands was constant.

We shall now consider a three-component mixture in order to establish the effect of a third component added to a two-component mixture. It should be borne in mind that the analytical amount of the original two components is equimolar and it is kept constant during the following treatment. There are two cases concerning the mobility order: $m_A > m_B > m_C$ or $m_C > m_A > m_B$. In the former the resolution time is expressed by eqn. 1 and in the latter it is expressed as follows [9]:

$$t_{res,AB} = \frac{l_B}{E_{AB}\bar{m}_{A,AB} - E_B\bar{m}_B} \quad (1)$$

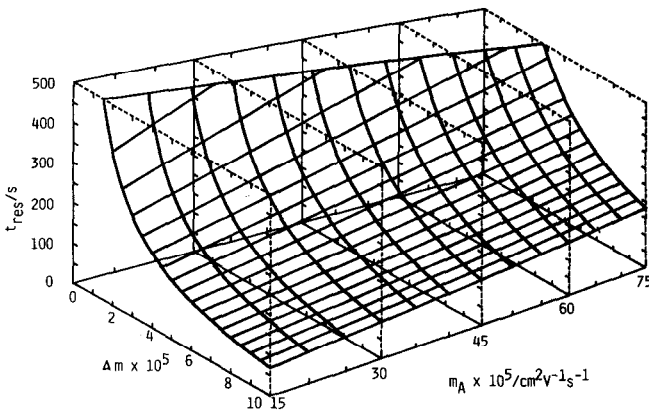


Fig. 2. Resolution time of an equimolar two-component mixture of model anions, A and B. Operational conditions as in Fig. 1.

As shown later, the extent of the increase in the resolution time with the addition of the third component was similar in both cases. However, it should be noted that the direction of the change of E_{AB} that causes the increase is different in the two cases.

The concentration ratio of separands A and B in the mixed zone AB is exactly expressed as follows in both cases [9]:

$$\frac{C_{B,AB}^t}{C_{A,AB}^t} = \frac{F_1 \bar{m}_{A,AB} \bar{m}_{B,I} C_{B,I}^t}{F_2 \bar{m}_{B,AB} \bar{m}_{A,I} C_{A,I}^t} \quad (11)$$

$$F_1 = \frac{(\bar{m}_{C,ABC} - \bar{m}_{B,ABC})}{\bar{m}_{C,ABC} E_{ABC} - \bar{m}_{B,AB} E_{AB}} \quad (12)$$

$$F_2 = \frac{(\bar{m}_{C,ABC} - \bar{m}_{A,ABC})}{\bar{m}_{C,ABC} E_{ABC} - \bar{m}_{A,AB} E_{AB}} \quad (13)$$

where the subscript ABC denotes the three-component mixed zone. The only possibility of changing E_{AB} is to change the ratio $C_{B,AB}^t/C_{A,AB}^t$ from the value for the two-component mixture, because it causes a change in the conductivity of the mixed zone ($m_A \neq m_B$). Combining eqns. 11–13 and the following relationship between E_{ABC} and E_{AB} obtained from the moving boundary equation:

$$E_{ABC} = \frac{\bar{m}_{A,AB} C_{A,AB}^t}{\bar{m}_{C,ABC} C_{A,AB}^t + (\bar{m}_{A,ABC} - \bar{m}_{C,ABC}) C_{A,ABC}^t} \cdot E_{AB} \quad (14)$$

one can rewrite eqn. 11, inserting eqn. 14 into eqns. 12 and 13, as follows:

$$\frac{C_{B,AB}^t}{C_{A,AB}^t} = \frac{\bar{m}_A (\bar{m}_B - \bar{m}_C) C_{A,ABC}^t}{\bar{m}_C (\bar{m}_B - \bar{m}_A) C_{A,AB}^t + \bar{m}_B (\bar{m}_A - \bar{m}_C) C_{A,ABC}^t} \quad (15)$$

This non-linear equation can be solved by combination with eqn. 5 and the following assumption for an equimolar three-component mixture:

$$C_{A,ABC}^t = C_A^t/3 \quad (16)$$

Consequently, the following equation is obtained for the ratio of the concentrations:

$$\frac{C_{B,AB}^t}{C_{A,AB}^t} = \frac{C_A^t - C_{A,AB}^t}{C_{A,AB}^t} \equiv R_C \quad (17)$$

$$C_{A,AB}^t = \frac{-Q + SG(Q^2 - 4PR)^{1/2}}{2P} \quad (18)$$

$$SG = 1 \text{ for } \bar{m}_A > \bar{m}_B > \bar{m}_C; \quad SG = -1 \text{ for } \bar{m}_C > \bar{m}_A > \bar{m}_B$$

$$P = 3\bar{m}_C(\bar{m}_B - \bar{m}_A) \quad (19)$$

$$Q = 2(\bar{m}_A\bar{m}_B - 2\bar{m}_B\bar{m}_C + \bar{m}_A\bar{m}_C)C_A^t \quad (20)$$

$$R = -\bar{m}_B(\bar{m}_A - \bar{m}_C)C_A^t{}^2 \quad (21)$$

This ratio is referred to as R_C hereafter. The value of R_C was larger than 1 when $m_A > m_B > m_C$ and less than 1 when $m_C > m_A > m_B$.

Eqn. 4 is also valid for a three-component mixture. C_{AB}^t in eqn. 4 is expressed using the concentration ratio as follows:

$$C_{A,AB}^t = C_A^t/(R_C + 1) \quad (22)$$

Combination of eqns. 4 and 22 gives the potential gradient of the mixed zone AB formed in the separation process of the three-component mixture, $E_{AB}(3)$, as follows:

$$E_{AB}(3) = \frac{\bar{m}_A(R_C + 1)}{\bar{m}_A + \bar{m}_B R_C} \cdot E_A \quad m_A > m_B > m_C \quad (23)$$

$$= \frac{\bar{m}_B(R_C + 1)}{\bar{m}_A + \bar{m}_B R_C} \cdot E_B \quad m_C > m_A > m_B \quad (23')$$

$E_{AB}(3)$ is larger than $E_{AB}(2)$ in eqn. 9 when $m_A > m_B > m_C$ and smaller than $E_{AB}(2)$ when $m_C > m_A > m_B$. Consequently, the resolution time of the mixed zone formed in the separation process of the three-component mixture can be expressed as follows:

$$t_{res,AB}(3) = \frac{Fn_A}{i} (1 + m_Q/m_A) \frac{\bar{m}_A + R_C\bar{m}_B}{\bar{m}_A - \bar{m}_B} \quad m_A > m_B > m_C \quad (24)$$

$$= \frac{Fn_B}{i} (1 + m_Q/m_B) \frac{\bar{m}_A/R_C + \bar{m}_B}{\bar{m}_A - \bar{m}_B} \quad m_C > m_A > m_B \quad (24')$$

As R_C for the three-component mixture was larger than 1 when $m_A > m_B > m_C$ and less than 1 when $m_C > m_A > m_B$, it is apparent that $t_{res,AB}(3)$ was always larger than $t_{res,AB}(2)$. The ratio of the resolution time, R_t , is expressed as follows:

$$R_t = \frac{t_{res,AB}(3)}{t_{res,AB}(2)} = \frac{\bar{m}_A + R_C\bar{m}_B}{\bar{m}_A + \bar{m}_B} \quad m_A > m_B > m_C \quad (25)$$

$$= \frac{\bar{m}_A/R_C + \bar{m}_B}{\bar{m}_A + \bar{m}_B} \quad m_C > m_A > m_B \quad (25')$$

For a sample mixture consisting of four or more separands, the resolution time of the mixed zone AB is also given by eqn. 24, although the mathematical expression of R_C

become complicated. The essential fact is that the effect of the addition of the fourth component is smaller than that of the third component, as shown later.

The separation efficiency in isotachopheresis is defined as the current efficiency in the separation. Therefore, it is closely related to the molar amount of separated sample/electric charges in coulombs. Mikkers *et al.* [4,5] defined the separation number (S) to discuss the separation efficiency as follows:

$$S = \frac{F \cdot n_A}{i \cdot t} = \frac{F \cdot n_A}{i \cdot t_{\text{res,AB}}} \quad (26)$$

Inserting eqn. 24 into eqn. 26 gives the following different expression for S for the case when $m_A > m_B > m_C$:

$$S = \frac{m_A}{m_A + m_Q} \cdot \frac{\bar{m}_A - \bar{m}_B}{\bar{m}_A + R_C \bar{m}_B} \quad (27)$$

S decreases with the addition of the other components. It should be noted that S is independent of the migration current.

EXPERIMENTAL

Samples

The samples used were 4,5-dihydroxy-3-(*p*-sulphophenylazo)-2,7-naphthalene-disulphonic acid (SPADNS), monochloroacetic acid (MCA), picric acid (PA) and 2,4-dihydroxybenzoic acid (DBA). Except for MCA, these samples absorb visible light (SPADNS and PA) and UV radiation (SPADNS, PA and DBA). The sodium salt of SPADNS was purchased from Dojin (Tokyo, Japan) in the purest form and the other compounds were obtained from Tokyo Kasei (Tokyo, Japan) (extra-pure grade), and were used as received. Stock sample solutions (10 mM) were prepared by dissolving the compounds in distilled water.

In order to confirm the above estimation, the separation processes of the following three equimolar mixtures were observed individually and the resolution times were compared with each other: (1) SM = SPADNS–MCA, (2) SMP = SPADNS–MCA–PA and (3) SMPD = SPADNS–MCA–PA–DBA. The pH of these solutions was adjusted to 3.6 by adding β -alanine.

Apparatus

Instead of a fixed detection system with an array of 32 equidistant UV detectors arranged along a separation tube [13], an isotachopheretic analyser with a scanning UV spectrophotometric detection system was used [10]. A fused-silica capillary of O.D. 0.66 mm and I.D. 0.53 mm (Gasukuro Kogyo, Tokyo, Japan) as the separation tube was scanned repeatedly over a length of 32 cm and the UV signals (position spectra of migrating zones) were acquired. A linear head equipped with a stepping motor was used to move the assembly of a deuterium UV lamp and a silicon photodiode detector. The UV radiation from the deuterium lamp was passed through a UV glass filter ($\lambda_{\text{max}} = 330 \text{ nm}$). A single cycle of scanning took 7.025 s and 5333

photometric signals were acquired through an analogue-to-digital converter. The resolution was 0.06 mm per data point, which was sufficient to trace the separation process accurately. For data acquisition, an NEC (Tokyo, Japan) PC9801VX microcomputer was used (80286–80287, clock 10 MHz). All experiments were carried out at 25°C. The details of this apparatus have been described previously [10].

Operational electrolyte system

The concentration of the leading electrolyte (hydrochloric acid) was 5 mM. The pH was adjusted to 3.6 by adding β -alanine. The terminator was 10 mM caproic acid. Hydroxypropylcellulose (HPC, 0.2%) was added to the leading and terminating electrolytes to suppress electroendosmosis. The viscosity of the 2% aqueous solution is 1000–4000 cP at 20°C according to the specification. The sample solution was injected into the terminating electrolyte near the boundary between the leading and terminating electrolytes. The pH of the terminating electrolyte was also adjusted to 3.6 by adding β -alanine to ensure that the pH of the sample solution at the initial stage of migration was equal to the prepared value. The pH measurements were carried using a Horiba (Tokyo, Japan) Model F7ss expanded pH meter.

Simulation

Two different methods for the simulation of the transient state have been reported [8]. One is based on solving a set of partial differential equations applying a suitable approximation [14–17] and the other is a direct analytical method to solve several simultaneous equations which should be satisfied in the mixed zones [4,5,7,18]. Using the latter approach, we have recently established a calculation method for the simulation of the isotachophoretic transient state of a sample mixture consisting of up to six separands. Although the complexity of the computational procedure increased considerably with increase in the number of separands, the concept of the simulation on the basis of the MSPR model was essentially the same as that reported for a three-component mixture [9]. In the analysis of a six-component mixture consisting of ions A, B, C, D, E and F, for example, iterative calculations were made until the *RFQ* functions [1,7] of the mixed zones AB, ABC, ABCD, ABCDE and ABCDEF were less than 10^{-5} simultaneously, and the other zones were analysed successively.

Appropriate initial properties of the mixed zones such as the separand concentrations were necessary for the smooth convergence of the iterative calculation. For example, when the transient zones of six separands are analysed, the calculation starts from the analysis for the two-component mixture, next the three component mixture, and so on until finally the six-component mixture was analysed using the results for the five-component mixture as the initial values. Therefore, the time needed for calculation increased progressively with increase in the number of separands. The previous computer code SIPSr was rewritten in Microsoft QUICK BASIC (the program size was 400 kB, the essential part being 150 kB). By use of an NEC PC-9801RA2 microcomputer (CPU 80386, coprocessor 80387, clock 16 MHz), it took several seconds for the two-separand analysis and about 6 min for the six-separand analysis.

RESULTS AND DISCUSSION

Simulation

The resolution time of a two-component mixed zone in a three-component mixture was evaluated for model anions by varying the mobility and the molar amount of the third component. The mobilities of two of the three separands, A and B, were fixed at $50 \cdot 10^{-5}$ and $45 \cdot 10^{-5} \text{ cm}^2 \text{ V}^{-1} \text{ s}^{-1}$. The sample amount was equimolar (50 nmol). The mobilities and the amounts were fixed throughout this study. The leading electrolyte used for the simulation was 10 mM hydrochloric acid buffered at pH 6 by adding histidine. According to the simulation of the separation process for a two-component mixture, the concentration ratio R_C was unity (*i.e.*, $C_{A,AB}^I = C_{B,AB}^I$), the potential gradient E_{AB} was 88.80 V cm^{-1} and the resolution time ($t_{\text{res},AB}$) was 1387s (I.D. of the separation tube = 0.5 mm, migration current = $100 \mu\text{A}$). As discussed above, these characteristics of the mixed zone AB were affected by the addition of the third component. The mobility of the third component, ion C, was assumed to be in the range $70 \cdot 10^{-5}$ – $51 \cdot 10^{-5} \text{ cm}^2 \text{ V}^{-1} \text{ s}^{-1}$ ($m_C > m_A > m_B$) and $44 \cdot 10^{-5}$ – $10 \cdot 10^{-5} \text{ cm}^2 \text{ V}^{-1} \text{ s}^{-1}$ ($m_A > m_B > m_C$). It should be noted the formulation in this paper is limited to the latter case. The amount of ion C was varied as 25, 50, 100 and 200 nmol.

Figs. 3 and 4 show the simulated values of the concentration ratio R_C (eqn. 17) and the potential gradient of the mixed zone, $E_{AB}(3)$, in the mixed zone AB. As expected, the ratio R_C depended significantly on the mobility and the amount of the third component C. When $m_A > m_B > m_C$, R_C was always greater than 1, *i.e.*, $C_{A,AB}^I < C_{B,AB}^I$, and less than 1 when $m_C > m_A > m_B$. In both cases, the deviation of R_C from unity was large when C was large and m_C was close to m_A or m_B . The change in R_C led to a change in the specific conductivity of the mixed zone AB. As the migration current was kept constant ($100 \mu\text{A}$), the potential gradient E_{AB} varied with the conductivity of the zone. The curves in Fig. 3 and 4 are the best-fitted functions using tanh functions.

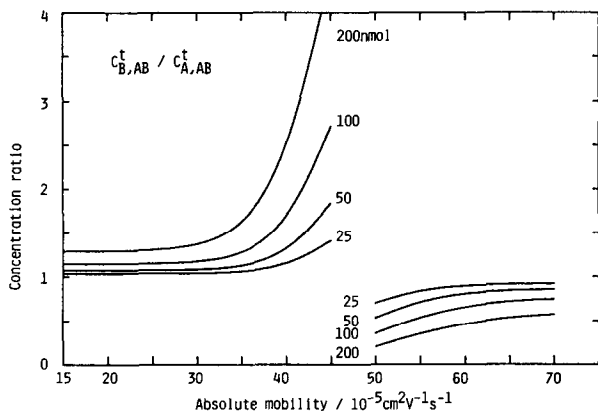


Fig. 3. Simulated dependence of concentration ratio $R_C = C_{B,AB}^I / C_{A,AB}^I$ on the molar amount and the mobility of the third component. The mobilities of two of the three separands, A and B, were fixed at $50 \cdot 10^{-5}$ and $45 \cdot 10^{-5} \text{ cm}^2 \text{ V}^{-1} \text{ s}^{-1}$ and the sample amount was equimolar (50 nmol). m_C = Mobility of the added third component, ion C. The I.D. of the separation tube was assumed to be 0.5 mm. Operational conditions as in Fig. 1.

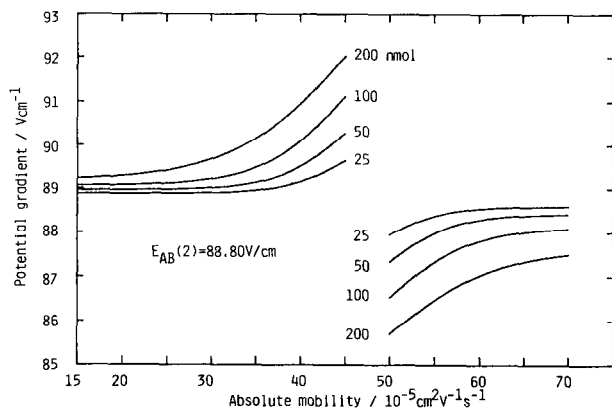


Fig. 4. Simulated dependence of the potential gradient of the mixed zone, E_{AB} , on the molar amount and the mobility of the third component. The I.D. of the separation tube was assumed to be 0.5 mm and the migration current was 100 μA . For other conditions see Fig. 3.

Fig. 5 shows the dependence of the increase in resolution time on mobility in terms of the ratio of resolution time R_t (eqn. 25). It should be noted that the increase was linear with respect to the molar amount of the third separand but not with respect to the mobility. Thus a large increase in the resolution time was observed when the mobility of the third separand was close to that of the original components. When 50 nmol of a component with a mobility of $51 \cdot 10^{-5} \text{ cm}^2 \text{ V}^{-1} \text{ s}^{-1}$ and $46 \cdot 10^{-5} \text{ cm}^2 \text{ V}^{-1} \text{ s}^{-1}$ was added to the original pair, respectively, the resolution time of the original pair was increased to 1943 s ($R_t = 1.40$) and 1884 s ($R_t = 1.36$). On the other hand, if the mobility of the third separand was far from that of the original sample, the increase in the resolution time was not as great.

Fig. 6 shows the separation diagrams simulated for the two- to six-component mixtures, which obey the separation diagram proposed by Brouwer and Postema [18].

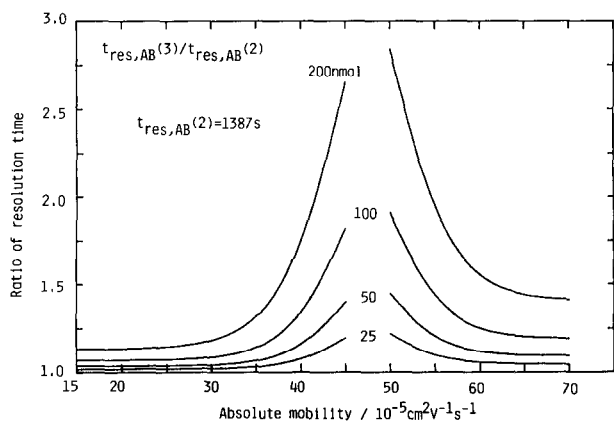


Fig. 5. Dependence of mobility on the ratio of resolution time, $R_t = (t_{\text{res,AB}}(3)/t_{\text{res,AB}}(2) \text{ of the three-component mixture})/t_{\text{res,AB}}(2) \text{ of the two-component mixture}$. See caption to Fig. 3. Operational conditions as in Fig. 1.

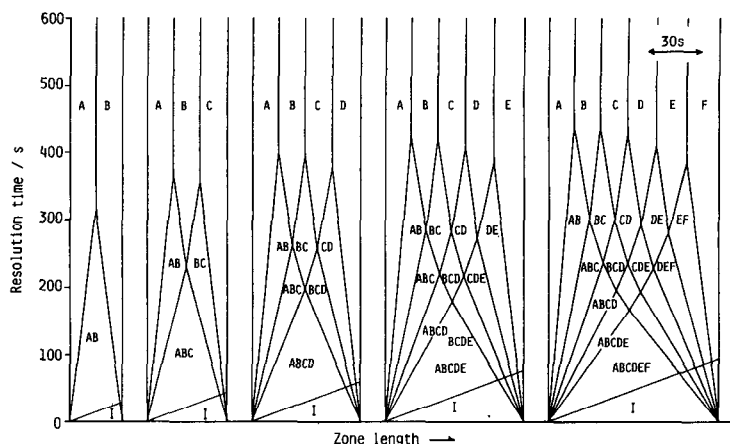


Fig. 6. Separation diagrams simulated for equimolar anions (A-F) with mobilities of $60 \cdot 10^{-5}$, $55 \cdot 10^{-5}$, $50 \cdot 10^{-5}$, $45 \cdot 10^{-5}$, $40 \cdot 10^{-5}$ and $35 \cdot 10^{-5} \text{ cm}^2 \text{ V}^{-1} \text{ s}^{-1}$. The $\text{p}K_a$ values were assumed to be -1 . The amount of each separand was 10 nmol . I represents the injected sample zone.

The mobilities of the model anions (A-F) were $60 \cdot 10^{-5}$, $55 \cdot 10^{-5}$, $50 \cdot 10^{-5}$, $45 \cdot 10^{-5}$, $40 \cdot 10^{-5}$ and $35 \cdot 10^{-5} \text{ cm}^2 \text{ V}^{-1} \text{ s}^{-1}$. The $\text{p}K_a$ values were assumed to be -1 . The concentration of the separands in the sample solution was 2 mM , the pH was 6 and the amount of the separands was 10 nmol . The operational electrolyte system was the same as that given in Table I. In Fig. 6, the leading and terminating zones are not shown and no mixing with samples was assumed. The potential gradients, the separand

TABLE II

RESOLUTION TIME OF SEVERAL MODEL ANIONS FOR TWO- TO SIX-COMPONENT MIXTURES

A-F = model anions with absolute mobilities of $60 \cdot 10^{-5}$, $58 \cdot 10^{-5}$, $53 \cdot 10^{-5}$, $48 \cdot 10^{-5}$, $43 \cdot 10^{-5}$ and $38 \cdot 10^{-5} \text{ cm}^2 \text{ V}^{-1} \text{ s}^{-1}$. The $\text{p}K_a$ values are assumed to be -1 . t_{res} = resolution time; $R_t = (t_{\text{res}} \text{ of two-component mixed zone in multi-component mixture})/t_{\text{res}}(2)$. Leading electrolyte: 10 mM HCl -histidine (pH 6).

Parameter	Mixed zone	No. of separands				
		2	3	4	5	6
t_{res}	AB	803	868	904	928	945
	BC	308	407	445	469	485
	CD	289		403	432	452
	DE	270			406	430
	EF	251				404
R_t	AB	1.00	1.08	1.13	1.16	1.18
	BC	1.00	1.32	1.44	1.52	1.57
	CD	1.00		1.39	1.49	1.56
	DE	1.00			1.50	1.59
	EF	1.00				1.61

concentrations, the resolution time, etc., of the two-component mixed zones are summarized in Table II together with those of the zones at the steady state.

Apparently from Fig. 6 and Table II, the resolution time of each two-component mixed zone increased with increase in the number of components in the mixture. Although this simulation is a special case for an equimolar mixture, the dependence of the resolution time on the number of components is easily calculated from the behaviour of R_1 in Fig. 5. Thus, the perturbation of the separation efficiency of the two components of interest caused by the addition of the other components can be discussed from the viewpoint of the number of separands in the mixture if the mixture is equimolar. When the mobility difference of neighbouring separands is appropriate, a considerable number of equimolar separands can be separated by isotachopheresis. For example, when the mobility of the terminating ion is $10 \cdot 10^{-5} \text{ cm}^2 \text{ V}^{-1} \text{ s}^{-1}$, that of the most mobile ion is $75 \cdot 10^{-5} \text{ cm}^2 \text{ V}^{-1} \text{ s}^{-1}$ and the mobility differences among the adjacent ions are $1 \cdot 10^{-5} \text{ cm}^2 \text{ V}^{-1} \text{ s}^{-1}$, a mixture of 65 anions (each 10 nmol) can be separated within 3200 s (migration current = 100 μA).

Observation of separation process

In order to confirm the present estimation, the resolution time of the two-separand mixed zone of SPADNS and monochloroacetic acid was measured for SPADNS, monochloroacetic acid, picric acid and 2,4-dihydroxybenzoic acid, and was compared with the results of simulation. Fig. 7 shows the transient isotachopherogram obtained with the scanning UV detector [10]. Fig. 7A shows the separation of SPADNS and monochloroacetic acid (concentration = 5 mM, volume injected = 5 μl), Fig. 7B that of SPADNS, monochloroacetic acid and picric acid (3.3 mM, 7.5 μl) and Fig. 7C that of SPADNS, monochloroacetic acid, picric acid and 2,4-dihydroxybenzoic acid (2.5 mM, 10 μl), referred to hereafter as SM, SMP and SMPD, respectively. The amount of each separand was the same (25 nmol). In these experiments, SPADNS and monochloroacetic acid corresponded to the model anions A and B.

The leading electrolyte was 5.00 mM hydrochloric acid- β -alanine (pH 3.6) and the migration current was 49.5 μA . In Fig. 7 one can see the increase in the resolution time of the SM zone: the observed resolution time for sample SM was 1030 s, that for SMP was 1141 s and that for SMPD was 1199 s. Table III summarizes the observed resolution times for the mixed zones formed in the separation process and the ratio with respect to two-separand mixed zones. Good agreement was obtained, confirming the present estimation. The method of evaluation of the resolution time and the boundary velocity was detailed in ref. 7.

In conclusion, the composition of the sample has a considerable effect on the separation efficiency of the two-component mixed zone of interest. To increase the separation efficiency, the amount of the coexisting components should be minimized, especially coexisting components having a similar mobility to the components of interest.

In the isotachopheretic analyser, a sample mixture is injected into the leading electrolyte or the terminating electrolyte. Apparently from Fig. 5, the mixing between the sample solution and the operational electrolyte should be minimized for a good separation efficiency. The present simulation was carried out on the assumption that the sample solution was injected ideally between the leading and terminating electrolytes, *i.e.*, the formation of a mixed zone between the samples and the leading

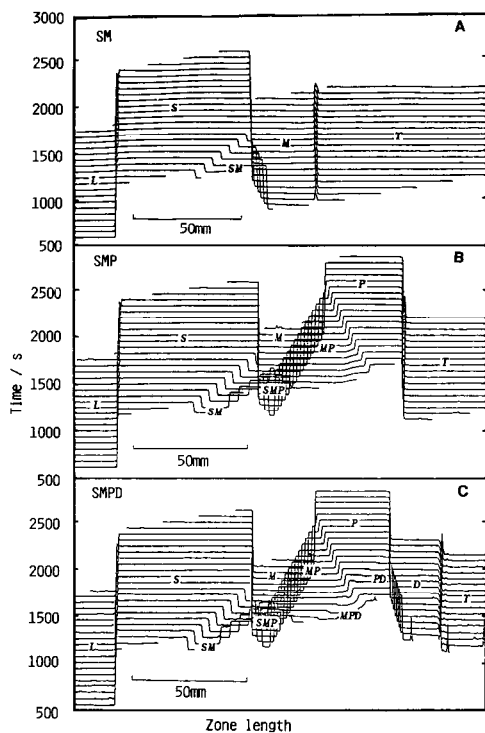


Fig. 7. Observed separation process of (A) SPADNS and monochloroacetic acid (concentration = 5 mM, volume injected = 5 μ l), (B) SPADNS, monochloroacetic acid and picric acid (3.3 mM, 7.5 μ l) and (C) SPADNS, monochloroacetic acid, picric acid and 2,4-dihydroxybenzoic acid (2.5 mM, 10 μ l) using the scanning UV detector. Leading electrolyte, 5.00 mM HCl- β -alanine (pH 3.6); terminating electrolyte, 10 mM caproic acid; migration current, 49.5 μ A.

TABLE III

RESOLUTION TIMES OF MIXED ZONES OBSERVED WITH THE UV SCANNING DETECTOR AND SIMULATED VALUES

S,M,P,D = sample anions: S = SPADNS; M = monochloroacetic acid; P = picric acid; D = 2,4-dihydroxybenzoic acid. The amount of each was 25 nmol. t_{res} = resolution time (s); figures in parentheses are simulated values; $R_1 = (t_{res} \text{ of two-component mixed zone in multi-component mixture})/t_{res}(2)$. Leading electrolyte: 5.00 mM HCl- β -alanine (pH 3.6). Migration current: 49.5 μ A.

Parameter	Mixed zone	Sample system		
		SM	SMP	SMPD
t_{res}	SM	1030 (1156)	1141 (1265)	1199 (1306)
	MP	—	1860 (1975)	1896 (1915)
	PD	—	—	1469 (1514)
	SMP	—	955 (1035)	1014 (1075)
	MPD	—	—	1110 (1153)
R_1	SM	1.00 (1.00)	1.11 (1.09)	1.16 (1.13)
	MP	—	1.00 (1.00)	1.02 (1.03)

electrolyte and a mixed zone between the samples and the terminating electrolyte was not taken into account. In an actual analysis, this will lower the separation efficiency.

In the separation of a multi-component mixture, it should be noted that the differences between the potential gradients of the separated adjacent zones were small (*ca.* 1 V cm^{-1} for the previous 65 model anions), and the difference may be much smaller in the separation process. This suggests that the self-restoring capability is low. Hence such a complex sample mixture may be easily perturbed by a flow along the capillary axis due to, for example, electroendosmosis.

ACKNOWLEDGEMENT

T.H. expresses his thanks to the Ministry of Education, Science and Culture of Japan for support of part of this work under a Grant-in-Aid for Scientific Research (No. 1540482).

REFERENCES

- 1 F. M. Everaerts, J. L. Beckers and Th. P. E. M. Verheggen, *Isotachopheresis—Theory, Instrumentation and Applications (Journal of Chromatography Library, Vol. 6)*, Elsevier, Amsterdam, 1976.
- 2 P. Bocek, M. Deml, P. Gebauer and V. Dolnik, *Analytical Isotachopheresis*, VCH, Weinheim, 1988.
- 3 T. Hirokawa, M. Nishino, N. Aoki, Y. Kiso, Y. Sawamoto, T. Yagi and J. Akiyama, *J. Chromatogr.*, 271 (1983) D1.
- 4 F. E. P. Mikkers, F. M. Everaerts and J. A. F. Peek, *J. Chromatogr.*, 168 (1979) 293.
- 5 F. E. P. Mikkers, F. M. Everaerts and J. A. F. Peek, *J. Chromatogr.*, 168 (1979) 317.
- 6 P. Bocek and P. Gebauer, *Electrophoresis*, 5 (1984) 338.
- 7 T. Hirokawa, K. Nakahara and Y. Kiso, *J. Chromatogr.*, 463 (1989) 51.
- 8 W. Thormann, *Sep. Sci. Technol.*, 19 (1984) 455.
- 9 T. Hirokawa, K. Nakahara and Y. Kiso, *J. Chromatogr.*, 470 (1989) 21.
- 10 T. Hirokawa, Y. Yokota and Y. Kiso, *J. Chromatogr.*, 538 (1991) 403.
- 11 T. Hirokawa and Y. Kiso, *J. Chromatogr.*, 260 (1983) 225.
- 12 R. A. Alberty, *J. Am. Chem. Soc.*, 72 (1950) 2361.
- 13 T. Hirokawa, K. Nakahara and Y. Kiso, *J. Chromatogr.*, 463 (1989) 39.
- 14 G. T. Moore, *J. Chromatogr.*, 106 (1975) 1.
- 15 M. Bier, O. A. Palusinski, R. A. Mosher and D. A. Saville, *Science*, 219 (1983) 1281.
- 16 V. Fidler, J. Vacik and Z. Fidler, *J. Chromatogr.*, 320 (1985) 167.
- 17 P. Radi and E. Schumacher, *Electrophoresis*, 6 (1985) 195.
- 18 G. Brouwer and G. A. Postema, *J. Electrochem. Soc.*, 117 (1970) 874.